ADVANCING LOCAL HELICITY INJECTION FOR NON-SOLENOIDAL TOKAMAK STARTUP

M.W. BONGARD, G.M. BODNER, M.G. BURKE, R.J. FONCK, J.L. PACHICANO, J.M. PERRY, C. PIERREN, J.A. REUSCH, A.T. RHODES, N.J. RICHNER, C. RODRIGUEZ SANCHEZ, C.E. SCHAEFER, J.D. WEBERSKI
University of Wisconsin-Madison
Madison, Wisconsin, United States of America
Email: mbongard@wisc.edu

Abstract

Robust non-solenoidal startup methods may simplify the cost and complexity of next-step burning plasma devices, and especially STs. Experiments on the $A \sim 1$ Pegasus ST are advancing the physics and technology basis of Local Helicity Injection (LHI). LHI creates high I_p tokamak plasmas by injecting helicity with small current sources in the plasma edge. Its hardware can be withdrawn before a fusion plasma enters a nuclear burn phase. Flexible injector placement offers tradeoffs between physics and engineering goals. They are tested with LHI systems on the low-field-side (LFS) and the high-field-side (HFS) of Pegasus, producing plasmas predominantly driven by non-solenoidal induction and DC helicity drive ($V_{LHI} \sim B_{inj}A_{inj}V_{inj}$), respectively. Record LHI plasmas with $I_p = 0.225$ MA, $T_e > 100$ eV, and $n_e \sim 10^{19}$ m^{-3} are attained. A predictive 0D power-balance model describes experimental $I_p(t)$ and partitions the active current drive sources. Analysis of experimental discharges with the model confirms the dominance of non-solenoidal induction in LFS LHI and DC helicity drive in HFS LHI. Studies of HFS scenarios find favorable, positive scalings of I_p with V_{LHI} and T_e with B_T. High-frequency MHD activity is found to be present during LHI current drive, in addition to $n = 1$ modes previously found in NIMROD simulation and experiment. A new regime of reduced MHD activity was discovered where $n = 1$ activity is suppressed, LHI CD efficiency improves, and long-pulse plasmas are sustained with $V_{IND} \sim 0$. LHI facilitates access to favorable ST regimes with non-solenoidal sustainment, high κ, low ℓ_i, and high β_t. Low B_T LHI operation has led to record $\beta_t = 100\%$, high β_N, and a minimum-$|B|$ well that may positively affect turbulence, transport, and fast particle confinement. Major facility upgrades are planned to extend LHI to higher I_p, B_T, and pulse length.

1. INTRODUCTION

Next-step burning plasma devices would strongly benefit from the availability of robust non-solenoidal startup techniques. By removing the need for a superconducting central solenoid magnet for inductive plasma initiation and ramp-up, smaller scale, lower cost devices with simplified nuclear shielding requirements may be realized. Such techniques are particularly relevant to burning spherical tokamaks (STs), which limit the available size and ramp-up capability of a solenoid magnet—if a solenoid is feasible at all [1]. Further, to be useful they must be compatible with the nuclear environment of the reactor and produce target plasmas that are compatible with subsequent non-inductive sustainment.

Several non-solenoidal startup techniques have been demonstrated that are envisioned to be compatible with future reactors. RF startup using electron cyclotron, lower hybrid, or electron Bernstein waves and/or DC helicity injection methods (Coaxial Helicity Injection (CHI) [2] and Local Helicity Injection (LHI) [3, 4]) have been tested on a variety of tokamaks and spherical tokamaks [5]. Outstanding issues for non-solenoidal startup include: attaining high I_p, density, and temperature; minimizing impurity production; producing targets with favorable MHD stability; and robust coupling to heating and current drive sources.

This paper describes experimental research results from the $A \sim 1$ Pegasus spherical tokamak [6] that are advancing the physics and technology basis of LHI. Pegasus is a university-scale ($R_0 \sim 0.4$ m, $a \sim 0.35$ m, $I_p \leq 0.3$ MA, $B_T \leq 0.15$ T) experimental component of the US ST research program.

2. LOCAL HELICITY INJECTION STARTUP ON PEGASUS

LHI produces tokamak plasmas without a solenoid by placing small electron current helicity injectors at the plasma boundary. They provide up to 1 kA/cm^2 from apertures with area A_{inj} of a few cm^2 at $V_{inj} \sim 1$ kV. High-performance sources extract electron current from an embedded, active arc discharge; passive and active, gas-effused electrode assemblies have also been tested for this purpose [7]. Force-free current is initially driven along vacuum field lines. Under appropriate conditions, this helical current stream relaxes through helicity-conserving magnetic turbulence to form a tokamak-like plasma with high current multiplication ($I_p/I_{inj} \geq 25$). (The “tokamak-like” state distinguishes a magnetic geometry that is fundamentally 3D in nature but has a

predominantly axisymmetric $n = 0$ tokamak structure [8, 9].) When helicity injection is complete, closed flux surfaces rapidly form [3, 9] and the resultant plasma may subsequently be sustained by other current drive methods. LHI-produced plasmas on Pegasus are compatible with Ohmic induction and attaining H-mode [10].

Flexibility in source location permits tradeoffs between poloidal field induction, helicity input, and physical access, which can be balanced by facility engineering constraints. Due to the small injector size for an LHI system, it could be inserted to initiate a tokamak discharge in a reactor and withdrawn from the vessel before the system enters a nuclear burn. Accordingly, this startup approach should place little burden on the nuclear system design requirements.

Access to the relaxed, tokamak-like state is first contingent on the production of a near-null in the vacuum poloidal field structure by the driven current streams [4, 11]. During this phase, the magnetic field geometry must provide sufficient pitch angle clearance for the injected current streams to avoid striking themselves following a toroidal transit (or other injector sets, in the case of toroidally-distributed injectors). Overhead in vertical clearance must be provided over vacuum field line following due to finite stream size, beam broadening along its arc length, kink motion of the line-tied current streams, and poloidal field reductions arising from I_{inj}.

The total I_p that can be driven by LHI in the relaxed phase is subject to the lower of two limits, given by

$$I_p \leq \frac{1}{2\pi\langle\eta\rangle}\left(\frac{A_p V_{loop}}{R_0} + \frac{N_{inj}A_{inj}V_{inj}}{R_{inj}}\right) \text{ or } I_p \leq \frac{\Psi}{\psi_{inj}} \approx \frac{\Psi I_{inj}}{2\pi R_{inj}B_p w} \rightarrow I_p \lesssim f_G\sqrt{\frac{\kappa\epsilon A_p I_{TF} I_{inj}}{2\pi R_0 w}}.$$

The helicity conservation limit (left equation) is due to balancing the current drive (helicity input) with resistive dissipation in steady state. Here A_p is the plasma area, V_{loop} is the inductive loop voltage, N_{inj} is the number of injectors, R_0 (R_{inj}) are the plasma (injector) major radii, and η is the plasma resistivity. The first term is inductive drive due to solenoidal induction, while the second represents an effective loop voltage V_{LHI} arising from helicity injection current drive [3, 4]. No discharges reported here employ a solenoid, and hence $V_{loop} = 0$.

The Taylor relaxation process imposes an absolute upper limit on I_p and reflects the lowest-energy Taylor state that conserves helicity on a resistive dissipation timescale [12]. This limit represents a constant magnetic inverse scale length $\lambda = \mu_0 J_\parallel / B$ across the plasma, with $J_\parallel$ the parallel current density and B the equilibrium magnetic field strength. When the poloidally-averaged edge $J_\parallel$ driven by the injectors is larger than the average core λ, turbulent fluctuations will relax the profile, transporting helicity into the core plasma, and drive I_p. This limit is expressed in machine parameters in the right equation above, with Ψ being the plasma toroidal flux, ψ_{inj} the injector poloidal flux, B_p the poloidal field at the injector, w is a radial distance at the outboard midplane representing the width of the turbulent, driven edge region, ϵ, κ are the inverse aspect ratio and elongation of the plasma, I_{TF} is the toroidal field rod current, and $1 < f_G < 2.5$ is a dimensionless function of plasma shape.

Two helicity injector systems are installed on Pegasus (Fig. 1) to examine the interplay between coupled physics and engineering considerations: a low-field-side (LFS) injector system sited below the outboard midplane ($N_{inj} = 3, A_{inj} = 2$ cm^2), and a new high-field-side (HFS) system in the inboard, lower divertor region ($N_{inj} = 2$, $A_{inj} = 4$ cm^2). These systems produce plasmas with drive dominated by non-solenoidal inductive drive [4, 9] and helicity injection [11], respectively.

The two injector systems on Pegasus feature complementary characteristics for purposes of LHI startup [13]. The LFS geometry has significantly simpler access to initial relaxation and strong inductive drive with respect to the HFS system, but declining values of helicity drive as the target plasma grows to its full-size geometry ($V_{LHI} \propto \Psi^{-1}$). In contrast, the HFS system: is more challenging to relax, due to pitch angle clearance considerations; has negligible to low inductive drive; and provides strong V_{LHI} with respect to the LFS system.

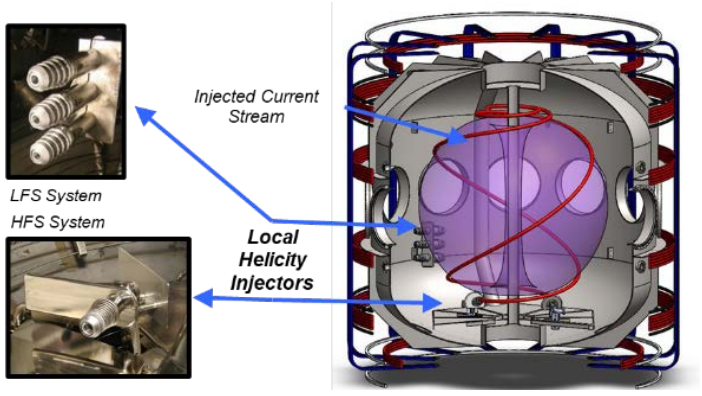


FIG. 1. Helicity injector systems on the Pegasus ST.

3. HIGH PERFORMANCE, NON-SOLENOIDAL LHI SCENARIO DEVELOPMENT

High performance LHI discharges have been developed that extend the range of attained I_p using the technique to a record 0.225 MA (peak $I_p = 0.240$ MA transiently attained) in a new scenario that combines helicity injection from both the LFS and HFS injector systems operating at the maximum $B_T = 0.15$ T in Pegasus. Figure 2 shows the I_p, I_{inj}, and V_{inj} waveforms from this discharge. The discharge is initiated by the LFS injectors and driven to ~0.1 MA at 25 ms. A strong poloidal field ramp is employed to detach the plasma from the LFS injectors, elongate the plasma, and couple to the HFS system as its power is increased to operational levels and I_p is increased. Helicity injection is terminated at 30 ms via a fast crowbar circuit. The produced plasma has a multi-ms decay after I_{inj} is extinguished. Performance in the low-current LFS phase was limited by available power supplies.

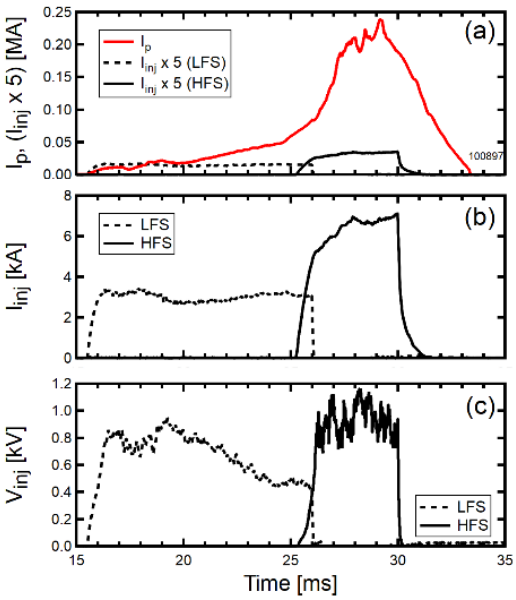


FIG. 2. $I_p > 0.2$ MA, $B_t = 0.15$ T plasma initiation via LFS → HFS LHI handoff.

Upgrades to the Pegasus multipoint Thomson scattering system [14] permit acquisition of radial profiles from $R = 0.18$ to 0.80 m utilizing 5–10 repeat discharges. Figure 3 shows such Thomson scattering measurements in the high current phase of the scenario of Fig. 2. The resultant plasma features peaked temperature, density, and pressure profiles, with $T_e > 100$ eV and core $n_e \lesssim 1 \times 10^{19}$ m^{-3}. These plasma parameters are comparable to those of Ohmic L-mode plasmas in Pegasus. Impurity line radiation identified from a SPRED VUV spectrometer system during LHI suggest oxygen and nitrogen are the dominant impurity species.

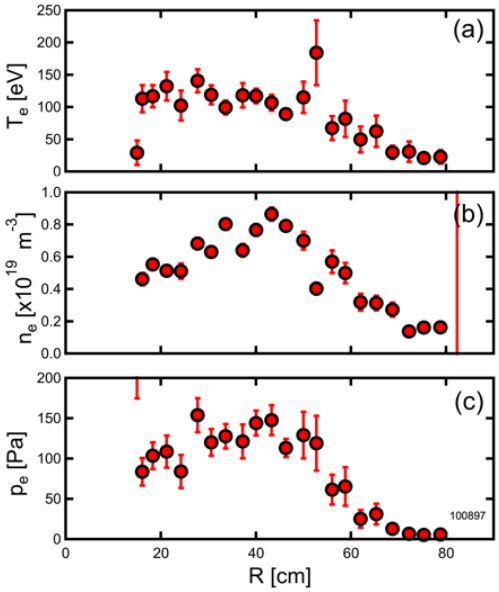


FIG. 3. Thomson scattering profiles of Fig. 2 discharge at 28.5 ms.

Attaining such performance and profile structure is not dependent on the use of the LFS → HFS handoff scenario. Similar plasmas with $I_p = 0.2$ MA and Thomson scattering profiles have been produced using the HFS injector system alone [11].

Direct measurement of Z_{eff} via VB measurements at these n_e and T_e levels is challenging, due to contaminating molecular and/or electron-neutral radiation in the spectral regions of interest [15]. An alternate means to infer impurity content in these plasmas is through a plasma resistivity analysis, under the assumptions that $R_p = V_{LHI}/I_p$, where R_p is an effective plasma resistance determined by experiment, and that resistive losses with neoclassical corrections are the dominant dissipation mechanism. 1D Thomson measurements are projected to 2D space using an equilibrium flux mapping. Trial $\eta_{NC}(R, Z)$ are calculated using these mapped Thomson data, a constant Z_{eff} treated as an unknown input parameter, and neoclassical resistivity formulations from Sauter [16]. This provides a secondary R_p estimate. Z_{eff} is then adjusted to obtain R_p values consistent with experiment. Application of this method to the well-diagnosed discharges in Figs. 2 and 3 implies $Z_{eff} \sim 1.7$. However, this estimate can vary significantly for other discharges. Hence, additional study of impurities is needed.

A brief operational campaign tested the potential to realize higher I_p using the LFS→HFS handoff scenario by relocating the HFS injectors from R_{inj}~26.1 to ~17.5 cm, such that V_{LHI} drive from the set increased by ~1.5×. This configuration proved to be outside the shape control capabilities of the present facility, as a more demanding placement of the lower foot of the plasma cross-section inboard of R_{inj} is required to obtain good coupling to the injectors and facilitate pitch-angle clearance of the injected current streams.

Figure 4 shows a representative discharge obtained in this campaign, in which the plasma foot was estimated to be at $R \geq R_{inj}$. Despite presenting the system with a slightly higher 0.1 MA initial target from the LFS injector set, poor coupling occurred and I_p growth was not realized. Additionally, the injector impedance was lower, likely due to higher neutral loads from the HFS injector streams intercepting local divertor rail limiter structures.

On a technical front, the successful high-performance LFS → HFS scenarios represent the first transfer of a helicity injected discharge from one LHI system to another with continuous growth in I_p. They also support extrapolation of LHI to devices with higher B_T, where optimal injector designs or operating points for obtaining initial relaxation to the tokamak-like state and consequent growth and sustainment may diverge from present experience, where a single injector system can perform both roles during LHI.

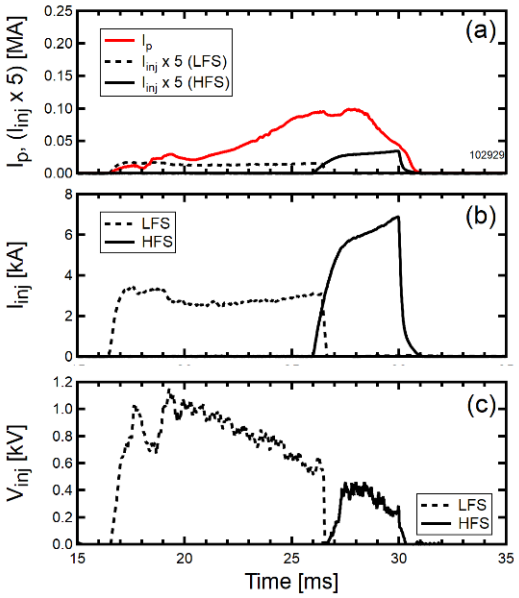


FIG. 4. $I_p \sim 0.1$ MA, $B_t = 0.15$ T plasma with poor LFS → HFS handoff coupling.

4. IMPROVING PREDICTIVE CAPABILITIES FOR LHI

The global Taylor relaxation and helicity balance limits provide upper bounds to the attainable I_p via LHI for a given facility and injector system. However, more sophisticated models are required to provide guidance on how LHI systems may be optimized for a desired target plasma configuration or how to navigate plasma growth from initial relaxation to the target configuration in a fashion that is compatible with shape control capabilities.

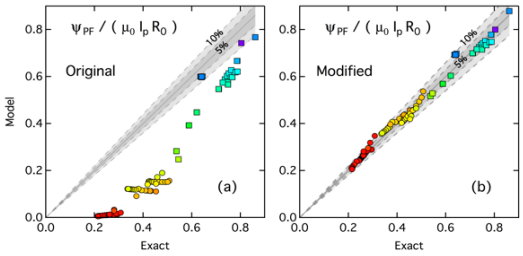


FIG. 5. Comparison of 0D power balance inductance models to equilibrium database with original (a), modified (b) inductance formulae. Adapted from [9].

As a first step towards addressing this need, a predictive 0D power-balance model using helicity conservation and Taylor limits for $I_p(t)$ was formulated [9]. Given prescribed, time-variable input terms representing the plasma position, shape, β_p and ℓ_i, helicity input (A_{inj}, V_{inj}, w), and a dissipative sink (*e.g.*, neoclassical resistivity), $I_p(t)$ is self-consistently calculated under the assumption that appropriate equilibrium field shape control is provided to realize the shape trajectory and enforce radial force balance. The analysis additionally quantifies the role of inductive voltages arising from shape changes, a moving plasma boundary, internal magnetic energy redistribution, and poloidal field induction as I_p is raised.

The partitioning of inductive drive voltages in the model relies on the accuracy of analytic formulae relating the plasma geometry to the equilibrium vertical field and external inductance [17]. A model equilibrium database was generated to test those analytic formulae in realistic plasma geometries [Fig. 5(a)]. Revisions to the inductive voltage terms were developed to provide correct models down to $A \sim 1$ [Fig. 5(b)]. A key uncertainty in the model is the treatment of its dissipative terms, which are strongly linked to confinement and T_e during LHI.

The improved model reproduces $I_p(t)$ trajectories to ~10% accuracy when using an approximate volume-averaged $\langle T_e \rangle$ for neoclassical plasma resistivity values in high I_p plasmas driven by both LFS and HFS injector systems (Fig. 6) [9, 11, 13]. The resultant

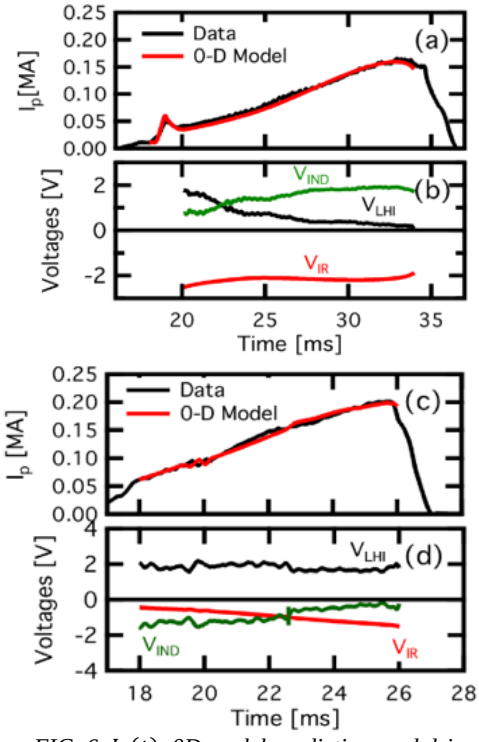


FIG. 6. $I_p(t)$, 0D model prediction, and drive voltages for LHI discharges with LFS (a), (b) and HFS (c), (d) injectors. Adapted from [13].

partitioning of the drive terms confirms the notion that LFS-driven LHI scenarios are predominantly driven by non-solenoidal induction that largely arises from plasma inductance changes ($V_{IND} > V_{LHI}$) and that HFS-driven LHI scenarios are predominantly driven by helicity injection ($V_{LHI} > V_{IND}$).

Despite the relative simplicity of the model, it affords predictions that inform scaling studies on Pegasus and a path to implementation on larger facilities like NSTX-U. In particular, manipulation of the early-phase Taylor limit early in LFS scenarios is projected to yield nonlinear gains in the final I_p, provided sufficient helicity input is available. (This input rate is strongly coupled with constraints from facility engineering requirements and injector source physics.) In contrast, simply increasing the available helicity input via $N_{inj}V_{inj}A_{inj}$ may offer only slight gains up to the baseline scenario's Taylor limit.

Model predictions using modest injector parameters ($A_{inj}V_{inj} = 20$ kV cm, $I_{inj} = 20$ kA) and conservative $\langle T_e \rangle \sim 150$ eV indicate $I_p \sim 0.8$ MA is feasible in NSTX-U geometry. Such an LHI injection system is only roughly a factor of two extension from present Pegasus injectors, and may feasibly be mounted on a single port.

5. SCENARIOS WITH MAJORITY LHI DRIVE

A major experimental focus in the 2016–18 run campaigns was the deployment and operation of the HFS helicity injector system [11]. This system doubled the injector current rating ($I_{inj} = 4$ kA/source) and quadrupled the V_{LHI} drive capability over the LFS system by doubling A_{inj} (4 cm^2/source) and siting the injectors at 3× higher B_T through their inboard location ($R_{inj} = 26$ cm).

The large-area arc injectors at high B_T support the scalability of the technology to larger, higher-field devices. Routine, reliable source operation with the injectors is attained up to the maximum $B_T = 0.15$ T on Pegasus, 10× over levels previously studied in this configuration.

Access to the relaxed, tokamak-like driven state is more challenging in this injector geometry due to the higher field, shorter path length along the field lines between injectors, and tighter alignment requirements. Aggressive use of vacuum field shaping and an injector arc power supply upgrade to supply $I_{arc} = 4$ kA/source were employed to facilitate relaxation at full B_T. A controlled study of relaxation requirements with these capabilities indicated that relaxation reliably occurs when the driven filaments' poloidal field significantly weakens the initial magnetizing field structure by 70–90% (Fig. 7), confirming prior studies [4] in LFS injector geometry that suggested the generation of a near poloidal null was required to attain relaxation.

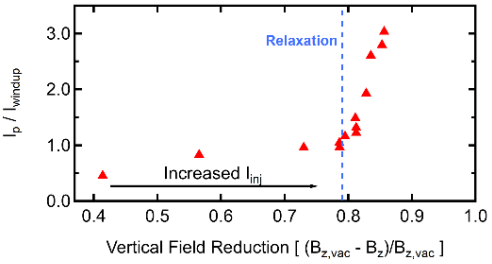


FIG. 7. Relaxation phase current multiplication as function of vacuum vertical field reduction [11].

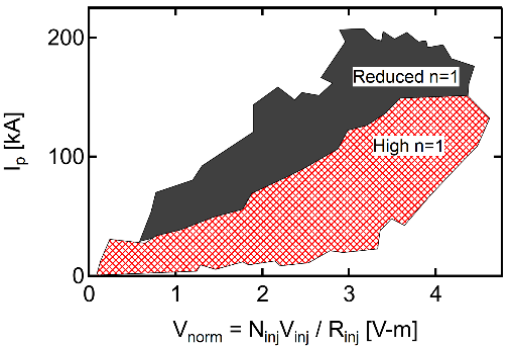


FIG. 8. I_p −normalized V_{LHI} operating space for 8,500 HFS LHI discharges. Higher performance occurs with mitigated $n = 1$ MHD activity [11].

With the HFS system, unwanted, deleterious plasma-material interactions were observed on lower divertor plates and local limiters with increasing frequency as B_T was increased. It often took the form of unipolar arcing on divertor plates and/or cathode spot instabilities [18] on the injectors. The former would degrade reproducibility, while the latter leads to termination of a discharge at its onset, due to its substantial impact on the effective injector area [9]. Such PMI is strongly influenced by the local electric field on the affected surfaces. It was mitigated by installing electropolished shield plates in the vicinity of the HFS injectors, as well as a set of local rail limiters to reduce the scrape-off layer density (and hence increase the Debye length that screens V_{inj} in the vicinity of the injectors). In addition, real-time cathode spot detection circuits were developed to rapidly terminate a failed discharge due to PMI onset. This significantly reduces lost run time due to reconditioning of the high-potential injector surfaces from these microscopic, explosive arc instabilities.

The HFS injector system was exploited to establish plasmas with $I_p \leq 0.2$ MA for $0.015 \leq B_T \leq 0.15$ T. This capability was used to gain insight into the realized confinement in plasmas sustained by helicity drive. Figure 8 shows the operating space spanned by over 8,500 HFS LHI discharges as a function of normalized injector voltage. In general, a favorable scaling is suggested, as the maximum realized current scales with available

drive voltage—and increases further in cases where $n = 1$ MHD activity is reduced, as discussed below. A scan of this space controlling for shape, constant $B_T = 0.05$ T, and with zero applied inductive voltage shows that I_p scales linearly with V_{LHI} (Fig. 9). This suggests that the effective plasma resistance is independent of helicity drive within these discharges. However, Thomson scattering profiles indicate that T_e varies by at least a factor of two in the discharges of Fig. 9. Additional experiments are needed to examine whether this trend is robust in longer-pulse, higher-B_T discharges and whether the losses are consistent with resistive helicity dissipation.

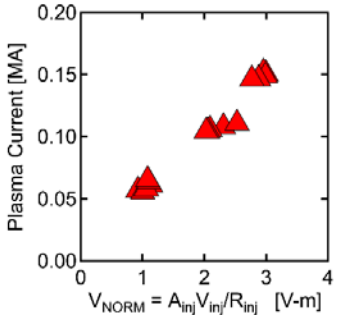


FIG. 9. I_p–V_{LHI} space for helicity-dominant plasmas. Adapted from [11].

6. ADVANCING LHI PHYSICS UNDERSTANDING

The physical mechanisms leading to LHI current drive generate strong MHD activity. Nonlinear, 3D resistive MHD NIMROD simulations of LHI startup have provided insight into dynamical processes observed in experiment and simulation [19], and spurred experimental investigations into MHD activity [13] and reconnection [20] during LHI.

These NIMROD simulations reproduced key features observed in Pegasus plasmas, including: toroidal current amplification following central column flux reversal; similar $I_p(t)$; the presence, spectral characteristics, and temporal evolution of low-frequency (~10s kHz) $n = 1$ activity on synthetic Mirnov coils in Pegasus geometry; and rapid flux surface closure following termination of LHI. They suggest a physical mechanism for the $n = 1$ activity: macroscopic reconnection of the helical injected current streams into axisymmetric "current rings" which then contribute to I_p growth. Such $n = 1$ activity is ubiquitous in LHI discharges [3, 4, 11, 13]. Internal and external magnetic measurements during LFS helicity injection experiments confirmed the $n = 1$ mode structure is consistent with that of a line-tied kink to the sources [13].

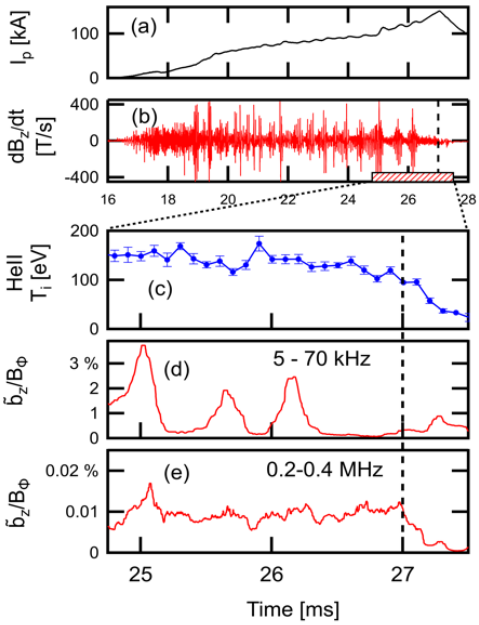


FIG. 10. LHI $T_i(t)$ correlated with continuous, high-frequency MHD activity [20].

Passive impurity Doppler spectroscopy indicated that the ion temperatures in LHI-initiated discharges was anomalously high, in that T_i routinely exceeds the central T_e [20]. Experiments confirmed that this anomalous ion heating is driven by strong magnetic reconnection activity present during LHI. $T_i(t)$ measurements as a function of direction with respect to the magnetic field without a background tokamak plasma show an anisotropic ion temperature distribution that scales in agreement with two-fluid reconnection theory. These experiments show reconnection-driven ion heating can arise from beams injected collinearly from adjacent edge sources, in addition to intra-stream helical passes. High time resolution $T_i(t)$ measurements during LHI (Fig. 10) showed that reconnection activity driving ion heating is best correlated with continuous, broadband, high-frequency MHD activity, and not the $n = 1$ bursts identified as a current drive mechanism in NIMROD.

New high-bandwidth magnetic probes [21] were developed to investigate such high-frequency activity. Fig. 11 shows an autopower spectrum obtained during LHI. Three main features are shown: a low-frequency $n = 1$ peak; a feature that appears ubiquitously near 700 ± 200 kHz; and an underlying continuum of broadband magnetic activity.

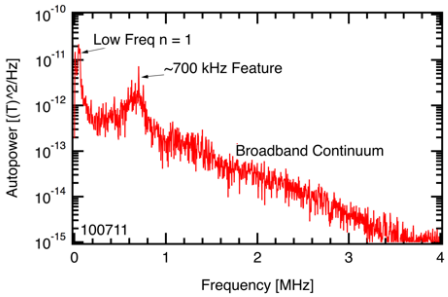


FIG. 11. High-bandwidth magnetic autopower spectrum with $n = 1$ mode and significant high-frequency content.

Initial experiments with the probes indicate that the 700 kHz feature arises from injector source physics, as it is present in the

presence of injector arc-only discharges and is spectrally coherent with injector V_{arc} and V_{inj} fluctuations. Fluctuations in the continuum frequency bands does not yield a well-determined n, and has radial coherence lengths of 3–5 cm. Characterization of the continuum as a function of LHI injector and plasma parameters is ongoing.

A new MHD regime was discovered using HFS LHI in which the $n = 1$ activity is rapidly and significantly reduced on the low-field-side of the vessel, leading to improved plasma performance [11, 13]. (It is not clear whether this reduction leads to improved current drive efficiency and/or reduced losses during LHI.) This reduction in $n = 1$ activity strongly suggests stabilization of the injected current streams. Figure 12 compares two discharges with identical field programming and LHI injector performance that is near the apparent threshold for this reduction event, which occurs near 21 ms. The underlying mechanism responsible for this significant event is unknown at present, and is the topic of considerable interest; if extensible to higher B_T, I_p, and n_e ranges expected in next-step machines then the performance enhancement may allow smaller-scale LHI systems to be deployed. To date, empirical dependencies of the reduction threshold include occurrence at I_p that increases with B_T (*i.e.*, with $I_p \sim I_{TF}$), neutral fueling, and applied V_{inj}. The $I_p \sim I_{TF}$ scaling and ready access to the reduced MHD regime at low B_T suggest the hypothesis that formation of a minimum-$|B|$ magnetic configuration may be a contributing factor to the transition [11].

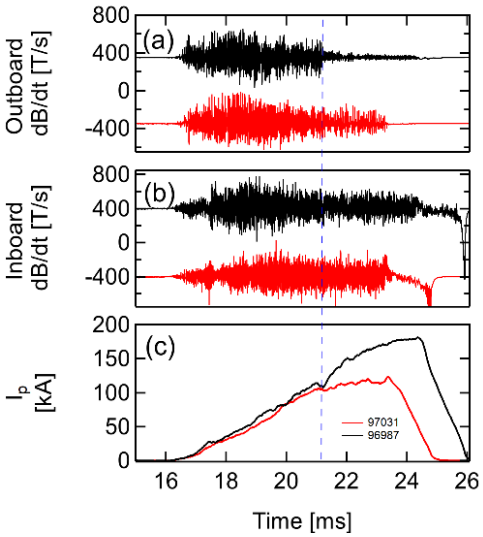


FIG. 12. Outboard, inboard $\dot{B}$ signals, and $I_p(t)$ for plasmas with and without a $n = 1$ MHD reduction event [11].

Long-pulse, $I_p = 0.1$ MA discharges sustained with zero measured poloidal field induction were produced in this low-MHD regime [11]. The pulse duration was limited only by available power supplies. This identifies the critical roles that short-scale MHD and reconnection activity play in LHI current drive.

Access to the reduced MHD state also facilitates access to the favorable low-A ST regime with non-solenoidal sustainment, high κ, low ℓ_i, and high β_t [22]. Non-inductively driven plasmas at low B_T access world-record $\beta_t \sim 100\%$, high $\beta_N \sim 6.5$ and feature an absolute minimum-$|B|$ magnetic configuration (Fig. 13) that may positively affect turbulence, transport, and fast particle confinement [23]. Discharges at highest β_t disrupt at the ideal no-wall MHD limit. Initial gyrokinetic simulations with GENE based on these LHI equilibria suggest the |B| well has a favorable impact on the stability of microtearing modes [24].

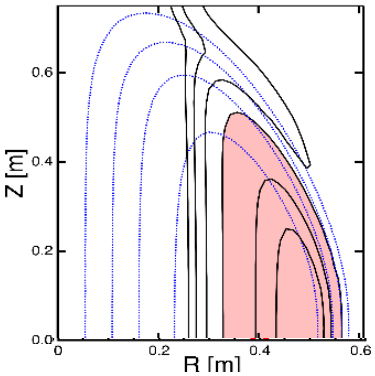


FIG. 13. $|B|$ contours (black), flux surfaces (blue) and min-$|B|$ region (red) in high-β_t plasma [23].

6. DISCUSSION

Continued progress in the physics and technology basis underlying non-solenoidal local helicity injection tokamak startup suggests that the method appears scalable to larger experiments such as NSTX-U and beyond. Critical open issues include extending LHI discharges to higher B_T, pulse length, and current, and improving our understanding of MHD and confinement in these discharges.

Major upgrades are planned to the Pegasus facility to test these issues, as well as support comparative studies with respect to non-solenoidal startup with CHI and the potentially synergistic effects of auxiliary RF heating and current drive. These upgrades will increase B_T 4× to 0.6 T, provide a diagnostic neutral beam for improved diagnostic capabilities, commission a new CHI startup system that does not require a vessel electrical break, and provide significant EBW heating and current drive capabilities.

ACKNOWLEDGEMENTS

This material is based upon work supported by the U.S. Department of Energy, Office of Science, Office of Fusion Energy Sciences, under Award Number DE-FG02-96ER54375. Disclaimer: Any opinions, findings, and conclusions or recommendations expressed in this publication are those of the authors and do not necessarily reflect the views of the U.S. Department of Energy.

REFERENCES

[1] MENARD, J.E. *et al.*, Fusion nuclear science facilities and pilot plants based on the spherical tokamak, Nucl. Fusion **56** (2016) 106023.

[2] NELSON, B.A. *et al.*, Demonstration of 300 kA CHI-startup current, coupling to transformer drive and flux savings on NSTX, Nucl. Fusion **51** (2011) 3008.

[3] BATTAGLIA, D.J., BONGARD, M.W., FONCK, R.J., REDD, A.J., SONTAG, A.C., Tokamak startup using point-source dc helicity injection, Phys. Rev. Lett. **102** (2009) 225003.

[4] BATTAGLIA, D.J., BONGARD, M.W., FONCK, R.J., REDD, A.J., Tokamak startup using outboard current injection on the Pegasus Toroidal Experiment, Nucl. Fusion **51** (2011) 073029.

[5] RAMAN, R., SHEVCHENKO, V.F., Solenoid-free plasma start-up in spherical tokamaks, Plasma Phys. Control. Fusion **56** (2014) 103001.

[6] GARSTKA, G.D. *et al.*, The upgraded Pegasus Toroidal Experiment, Nucl. Fusion **46** (2006) S603.

[7] FONCK, R.J. *et al.*, Local current injector system for nonsolenoidal startup in a low aspect ratio tokamak, Proc. 24th IAEA Fusion Energy Conference, San Diego, USA, no. FTP/P1-19.

[8] TANG, X.Z., BOOZER, A.H., Numerical studies of a steady state axisymmetric co-axial helicity injection plasma, Phys. Plasmas **11** (2004) 171.

[9] BARR, J.L. *et al.*, A power-balance model for local helicity injection startup in a spherical tokamak, Nucl. Fusion **58** (2018) 076011.

[10] THOME, K.E. *et al.*, H-mode plasmas at very low aspect ratio on the Pegasus Toroidal Experiment, Nucl. Fusion **57** (2017) 022018.

[11] PERRY, J.M. *et al.*, Initiation and sustainment of tokamak plasmas with local helicity injection as the majority current drive, Nucl. Fusion **58** (2018) 096002.

[12] TAYLOR, J.B., Relaxation and magnetic reconnection in plasmas, Rev. Mod. Phys. **58** (1986) 741.

[13] REUSCH, J.A. *et al.*, Non-inductively driven tokamak plasmas at near-unity β_t in the Pegasus Toroidal Experiment, Phys. Plasmas **25** (2018) 056101.

[14] SCHLOSSBERG, D.J. *et al.*, A novel, cost-effective, multi-point Thomson scattering system on the Pegasus Toroidal Experiment (invited), Rev. Sci. Instrum. **87** (2016) 11E403.

[15] ANDERSON, J.K. *et al.*, Direct removal of edge-localized pollutant emission in a near-infrared bremsstrahlung measurement, Rev. Sci. Instrum. **74** (2003) 2107.

[16] SAUTER, O., ANGIONI, C., LIN-LIU, Y.R., Neoclassical conductivity and bootstrap current formulas for general axisymmetric equilibria and arbitrary collisionality regime, Phys. Plasmas **6** (1999) 2834.

[17] HIRSHMAN, S.P., NEILSON, G.H., External inductance of an axisymmetric plasma, Phys. Fluids **29** (1986) 790.

[18] ANDERS, A., Cathodic Arcs, Springer Series on Atomic, Optical, and Plasma Physics No. 50, New York (2008).

[19] O'BRYAN, J.B., SOVINEC, C.R., Simulated flux-rope evolution during non-inductive startup in Pegasus, Plasma Phys. Control. Fusion **56** (2014) 064005.

[20] BURKE, M.G. *et al.*, Continuous, edge localized ion heating during non-solenoidal plasma startup and sustainment in a low aspect ratio tokamak, Nucl. Fusion **57** (2017) 076010.

[21] RICHNER, N.J. *et al.*, Radially scanning magnetic probes to study local helicity injection dynamics, Rev. Sci. Instrum **89** (2018) 10J103.

[22] ONO, M., and KAITA, R., Recent progress on spherical torus research, Phys. Plasmas **22** (2015) 040501.

[23] SCHLOSSBERG, D.J. *et al.*, Noninductively driven tokamak plasmas at near-unity aspect ratio, Phys. Rev. Lett. **119** (2017) 035001.

[24] SMITH, D.R. *et al.*, Microstability properties of the local minimum |B| regime in Pegasus, US Transport Task Force Workshop, San Diego, CA, USA (2018).